# *Experimental damage analysis of concrete structures using the vibration signature - Part I: diffuse damage (porosity)*

Z. Boukria, A. Limam

***Abstract*—**This paper reports on an experimental non-destructive method for characterizing the damage of concrete structures using the vibration signature. The frequency of the material is an indicator of damage to the structure. Pathologies such porosity induces stiffness degradation in the concrete and thus causes damage. The determination of the elastic modulus and resistance characteristics of specimens through bending and compression tests is used to study the variation of dynamic modulus during cycles of wetting and drying (porosity).

***Keywords*—**Diffuse damage, concrete, porosity, vibration frequency, elastic modulus.

## I. INTRODUCTION

FOR the safety of civil engineering structures, periodic testing is necessary. It is important for the engineer to ensure that buildings are capable of performing their function. This is possible through the detection of any weaknesses over time and the subsequent orderly planning of necessary interventions. In order to monitor these structures, it is important to be able to identifying their condition [1,2,3].

Concrete damage is the major problem for this type of structure. Its characterization has been treated by several authors using a physical model [4,5,6] such as Mazars' isotropic model [7] based on Kachanov's variable of [8]. Other authors have used non-destructive methods: dynamic testing [9,10] where the principle is to analyze the changing of dynamic characteristics [11,12,13] in the presence of damage, ultrasonic methods [14,15] based on wave propagation, or a combination of several methods [16].

Concrete is a composite material composed of aggregates of different sizes, a cement matrix and cavities. It presents randomly distributed micro-cracks which are present prior to any external stress. Depending on the nature and intensity of the stress, concrete deformation is complex [17,18] involving one or more combinations of basic mechanisms: elasticity, damage, sliding friction and cracking. This makes it difficult to find a physical model to represent these fracture modes and crack propagation that is reliable and easy to use.

This study is based on damage analysis using vibration signatures. The various methods for vibrating structures to identify the natural frequencies of a building are easy to implement (non-destructive methods). The objective is to periodically determine the "vibration signature" of the studied specimens and correlate any changes in them subsequent to a loss in strength.

The diffuse damage of a material can be characterized by its porosity [19]; for concrete this porosity is represented by the relation W / C (water / cement) [17,20].

## II. APPROACH

The method is based on studying dynamic modulus (Young and shear) [21,22] over time as well as diffuse defects on specimens. It consists of vibrating a cured concrete specimen, measuring the resonant frequency with Grindosonic [23] and calculating the dynamic modulus of elasticity of the specimen with the obtained results.

The GrindoSonic (Fig. 1) is a device for measuring the elastic properties of materials using a dynamic method. The speed and simplicity of these non-destructive measurements means that they can be repeated without limitation on the same specimen to observe changes over time.

The instrument uses the excitation pulse technique [24] to dynamically determine the elastic modulus of materials.

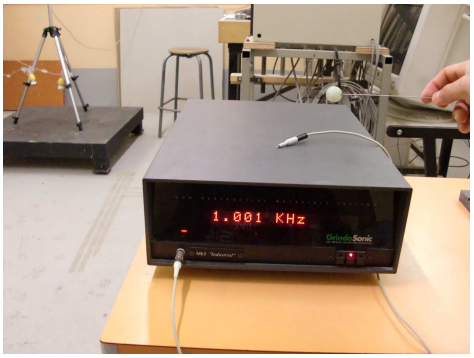


Fig. 1 Grindosonic

The operation consists of exciting the object with a light mechanical impulse and to analyze the resulting transient vibration. The natural vibration is determined by the geometry and physical properties of the specimen. A piezoelectric sensor

(or microphone) is used to sense the mechanical vibration and convert it into an electrical signal. An electronic circuit detects the zero crossing, accurately marking the successive periods. As the signal decreases, the instrument measures each period and keeps the value in memory. This continues until the virtual extinction of the signal. Finally, the microprocessor analyzes the stored information, selects the fundamental component of the spectrum and displays the measurement result.

This result may appear in 3 forms: i) the traditional reading (R) which gives the duration of two periods of the fundamental vibration, expressed in microseconds; ii) the new reading (T), which also gives the length of two periods but in a constant resolution format (this format requires the use of commas and display units on milliseconds or microseconds) and iii) the frequency (F) expressed in hertz or kilohertz.

There is a very simple relationship between reading (R or T in µs) and frequency (F in Hz):

F = 2,000,000 / R

There are three steps to performing a test: placing the sensor, impacting the specimen, and reading the measurement.

The positions of the piezoelectric sensor, the impact and the support can all be changed according to the different resonance modes.

The following figure (Fig. 2) summarizes the procedure for each mode of vibration and the formula for calculating the Young's modulus.

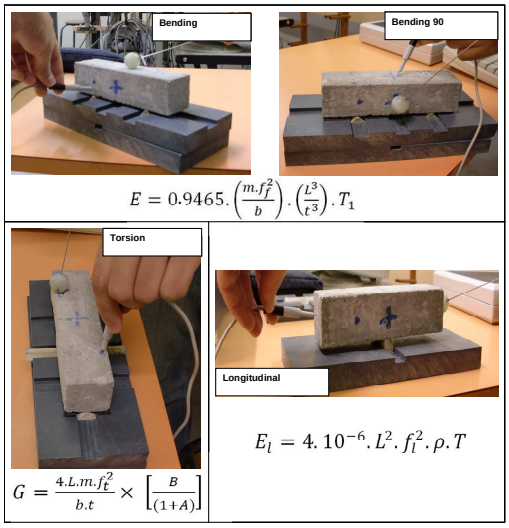


Fig. 2 Measurement of Young's modulus by Grindosonic

With this method, measurements can be made on all solid materials as long as the internal friction does not exceed a certain limit. The dimensions and shapes of objects measured can vary widely, ranging from small bars measuring 3 x 4 x 40 to concrete beams weighing over a ton.

## III. EXPERIMENTAL SET-UP

### A. *Specimens*

To fabricate the specimens measuring 40x40x160cm, the materials are: ISO 679 standard sand and cement CEM I 52.5 PM CP2. For materiel quantities, the standard NF EN 196-1 [25] was respected: 450 g ±2g of cement, 1 350 g ±5g of sand, 225 g ±1g or water.

Adjuvants used were an anti-withdrawal and water-retaining polycarboxylate superplasticizer, two viscosifying agents (polyvinyl alcohol and Wellan gum) and a retarder.

The different specimens (Fig 3) were tested in accordance with American standard ACTM C1259-01. For tests using GrindoSonic, only the first 10 test values were retained. The frequency of the test (bending, bending 90°, longitudinal, torsion) was calculated by averaging the 10 measurements. For each frequency, the interval was calculated by from the upper bound: {Mean + standard deviation} and the lower bound: {Mean - standard deviation}. This explains the presence of moduli of ± S in the figure.

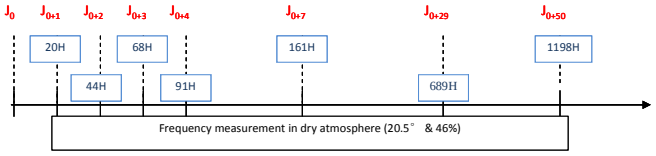


Fig. 3 Specimen series and measurement planning

8 sets of 3 specimens were manufactured in accordance with standard EN 196-1, by varying the water-cement ratio (Table. I). The first set of tests used the ratio recommended by the standard (defined as the baseline report) and then, for each set of tests, 1% water was added during their manufacture until the maximum value of 9% (series 6 and 8% were not carried out).

| **Series** | $E_0$ | $E_1$ | $E_2$ | $E_3$ | $E_4$ | $E_5$ | $E_7$ | $E_9$ |
|---|---|---|---|---|---|---|---|---|
| **W/C** | $E_{ref}$ | $E_{ref+1\%}$ | $E_{ref+2\%}$ | $E_{ref+3\%}$ | $E_{ref+4\%}$ | $E_{ref+5\%}$ | $E_{ref+7\%}$ | $E_{ref+9\%}$ |

Table. I W/C for specimen series

### B. *Wet- Dry cycle*

Tests were conducted on a specimen series, from E0 to E9. They were placed on a metal grid and immersed in a tank filled with water at 20° for 14 days before testing. The procedure was to:

- dry the speciment test Eij "Wet" (i = % additional water relative to the reference specimen, j = 1,2 or 3; it differentiates the three specimens cast in the same mold)
- note the date, time, humidity and temperature of the room,
- weigh the specimen to 100th of a gram
- visually inspect the surfaces of the specimen and note any defects such as cracks and chips
- place the specimen precisely on the support as required for the desired frequency
- start the vibration of the specimen using the adapted impact hammer and repeat the process at least 10 times and until three identical values near ± 30 HZ
- note the average of the values obtained and calculate the dynamic Young's modulus with the GEMOD programme or the NBN-B 15-230 standard [26]

let the specimen dry vertically for 12 hours and then repeat the procedure; continue the process until the modulus calculated before immersion is reached.

### C. *Dry-wet cycle*

The same procedure as for the dry / wet cycle is applied to the specimens before immersion. After obtaining all the results, specimens are immersed for about 12 hours and then tested tried. The procedure is repeated for 15 days minimum to obtain representative and exploitable results.

## IV. RESULTS

The aim of this test is to monitor the dynamic moduli of specimens in a dry atmosphere during the first days of casting and until day 28, and then to check (using the vibration method), by observation, for the presence of diffuse defects (in this case, porosity) with the dynamic modulus results.

All moduli in bending and bending 90 were identified using a Poisson's ratio calculated with an iterative method; it is therefore not constant in any particular specimen. In all tests the value of Poisson's ratio varied from 0.05 to 0.21.

To control the influence of Poisson's ratio on the results, all calculations were repeated with ν = 0.2 and the largest gap on greatest difference with the average dynamic modulus was 292 MPa (the average value being 141 MPa).

### A. *The dynamic modulus over times*

For each test series, the dynamic moduli are calculated for all time steps.

After casting Figure 4 shows an example of modulus change over time (with a logarithmic base of 10) for specimen E9. These curves are representative of the majority of test series. There is a very strong increase until hour 44, then very little change until hour 161 and finally a slight decrease in modulus.

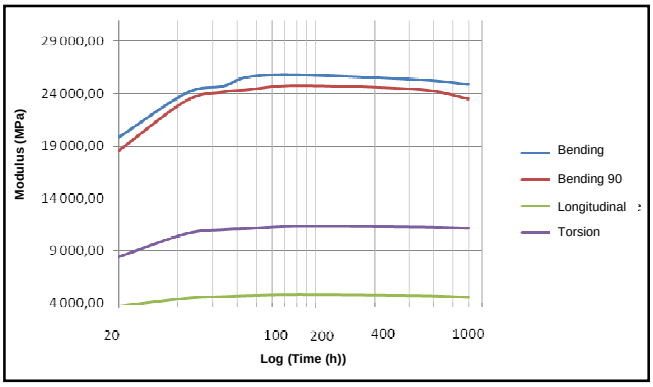


Fig. 4 Modulus change over time, specimen E9

These three stages can be explained as follows:

- The strong increase of modulus until the 44th hour: the specimen is tested for the first 20 hours after casting out of its protective plastic in a high humidity environment in which only very small amount water within the mortar could evaporate. Storing the specimens in a dry atmosphere and at a temperature of 20°C causes a sudden rise in mortar strength and acceleration in cement hydration. The cement used was a CEM I 52.5 PM CP2 with 63.4% of C3S, an average strength of 36 MPa after 2 days (48h) and 62% of its average strength at 28 days.

- Modulus does not vary until hour 161: with a pseudo-equilibrium between the hydration of cement and the increasing strength of the specimens, the modulus increases much more slowly.

- Drop in dynamic modulus after hour 161: the hydration water having reacted "fully," the water molecules that have been consumed and leave spaces, that increase porosity, lowering the modulus.

Only series E3 and E4 differ from this format, since their modulus decrease from hour 689 and then rise again at hour 1198; for the second series, the modulus does not vary from hour 161. This variation in the format is due to use modulus averages (the frequency considered is the average frequency of 3 series of tests) and the last test (hour 1198) is performed with a single specimen.

### B. *Comparison of specimens' dynamic modulus based on the rate of default diffuse (percentage porosity)*

Using the same results, it is possible to compare these sets of specimens to determine whether GrindoSonic can easily identify and quantify the level of porosity in materials. The following figures (Fig. 5 and Fig. 6) show modulus change over time (bending and torsion)

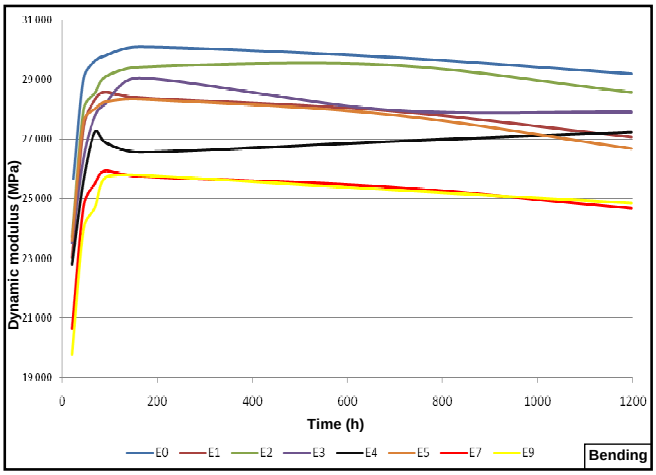


Fig. 5 Modulus change (over time) in bending for all tests

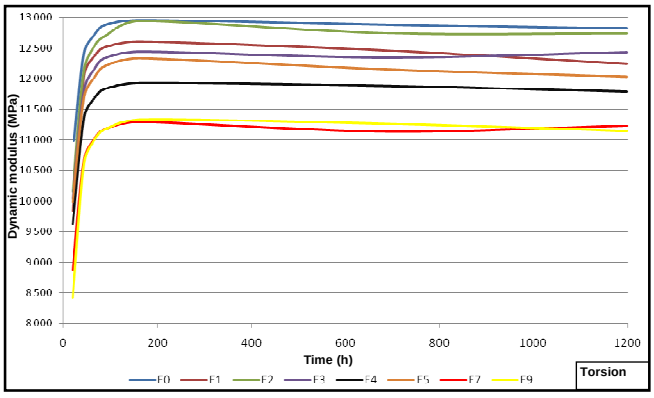


Fig. 6 Modulus change (over time) in torsion for all tests

Only graphs of dynamic modulus in bending and torsion are shown here. The conclusions are identical for the two other dynamic moduli (longitudinal and bending 90) and they do not provide any additional information. The dynamic modulus decreases more or less depending on the porosity; the following figure (Fig. 7) shows this evolution for a given test.

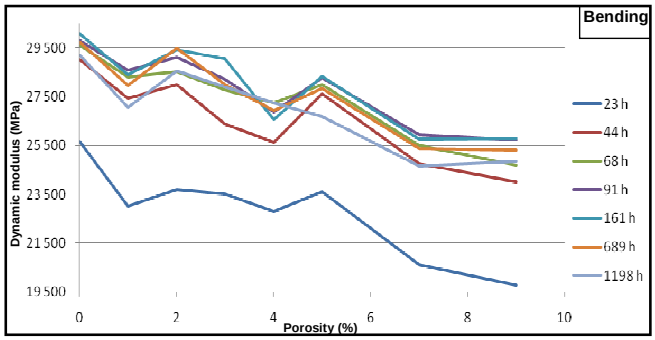


Fig. 7 Comparison of modulus / porosity

The curves remain the same whatever the calculated dynamic modulus (bending 90, torsion and longitudinal). Using these results, it is possible to combine different sets of specimens in 3 separate groups by classifying modulus from the highest to the lowest: the first group includes sets E0 and E2, the second group, the series E1, E3, E4, E5 and the third group, series E7 and E9. It is difficult to distinguish between sets of the same group because one must take into account the uncertainties of measurements and calculations of all averages (average frequency and average modulus of the series).

In order to find the average difference of modulus and frequency between the three groups of series, average deviations of the results found upstream in the reference series E0 are calculated (Table. II). All the results initially depend on the dynamic modulus average found in 3 specimens of each series. When comparing each specimen to the average of its series, there is necessarily a greater or lesser difference which becomes an uncertainty in the comparison between the series.

| Average | Bending | | Bending 90 | |
|---|---|---|---|---|
| | Modulus (MPa) | Frequency (Hz) | Modulus (MPa) | Frequency (Hz) |
| $E_2$ | 902 | 113 | 273 | 67 |
| $E_1$, $E_3$, $E_4$, $E_5$ | 2 046 | 172 | 2 122 | 189 |
| $E_7$, $E_9$ | 4 529 | 372 | 4 986 | 414 |
| | Torsion | | Longitudinal | |
| | Modulus (MPa) | Frequency (Hz) | Modulus (MPa) | Frequency (Hz) |
| $E_2$ | 241 | 105 | 188 | 114 |
| $E_1$, $E_3$, $E_4$, $E_5$ | 733 | 198 | 383 | 172 |
| $E_7$, $E_9$ | 1 785 | 463 | 901 | 390 |

Table. II Average difference of modulus

It is interesting to study the impact of uncertainties for the time step of hour 689 (28 days), since the results are more stable and the mortar has reached its characteristic resistance.

The following graph (Fig. 8) represents the uncertainties, for each series (E0, E1, E2 etc.) tested in bending, as black lines and the position of the modulus as a red triangle. All results are expressed as variations of the dynamic modulus (%) using series E0 as reference.

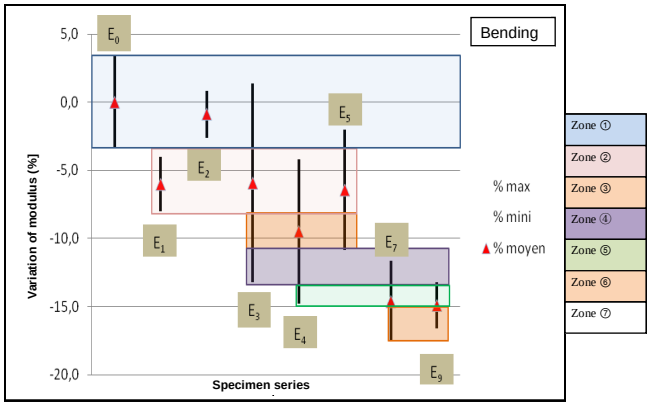


Fig. 8 Variation of modulus and uncertainties in relation to reference series E0

Seven different zones are detailed in the following table (Table. 3**)** which represents changes in dynamic modulus for bending 90, torsion and longitudinal. Using these measurement intervals, and after vibration tests in all directions (bending, bending 90, torsion and longitudinal) on a 40x40x160 mm specimen, it is possible to determine the diffuse damage of the specimen and to place it in a group. For example, for series E3, the results of the test are summarized in Table 5.

| Series | Bending E (MPa) | Bending 90 E (MPa) | Torsion G (MPa) | Longitudinal E (MPa) |
|---|---|---|---|---|
| $E_0$ | 29 748 | 29 311 | 12 887 | 5 676 |
| $E_3$ | 27 984 | 27 545 | 12 348 | 5 282 |
| Variation (%) | -5.9 | -6.0 | -4.2 | -6.9 |

Table. III Variation of dynamic modulus for series E3

Using the previous table, specimens can be classified as Series E1, E3, E4 and E5 and in the Table 4 this interval is restricted to E1, E3 and E5. This method is not perfect because it is not easy to find the exact value of the porosity (diffuse damage) but it is possible to place it within a specified interval. However, if the specimen is older or younger the results are more random.

### *C. Wet-dry cycle*

After immersing a specimen of each series in a water bath for 14 days, GrindoSonic tests were performed to determine the changes in frequencies and dynamic modulus in the four "directions during the evaporation of the water that had been absorbed by the specimen. Between two measurements, the specimens were stored vertically in an air-conditioned location (humidity and temperature averages were, respectively, 37.9% and 22.3°).

The tests showed that the values of the weights, frequencies and modulus varied very little, so measurements were spaced (Fig. 9), each time taking into account the speed of change of the three criteria mentioned above.

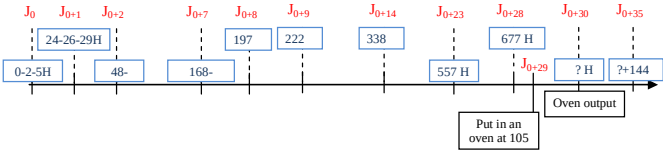


Fig. 9 Dates of measurements in the wet-dry cycle

The table below (Table. IV) shows the differences in the 3 criteria (weight, frequency and modulus) before wetting and after the 29th "dry" day.

| Series | Differences on Weight (g) | Deviation of frequency and dynamic modulus | | | | | | | |
|---|---|---|---|---|---|---|---|---|---|
| | | FF | E (MPa) | FF90 | E (MPa) | FT | G (MPa) | FL | E (MPa) |
| E02 | 11.9 | 508.0 | 6 998.5 | 550.8 | 7 597.1 | 678.9 | 2 929.2 | 536.9 | 1 385.3 |
| E13 | 11.9 | 550.5 | 7 947.9 | 578.8 | 8 608.4 | 723.7 | 3 198.9 | 552.1 | 1 456.3 |
| E22 | 12.6 | 532.4 | 7 302.9 | 533.3 | 7 431.5 | 710.6 | 3 078.1 | 542.5 | 1 404.3 |
| E32 | 12.7 | 554.0 | 7 477.7 | 566.2 | 7 746.3 | 738.3 | 3 150.8 | 548.0 | 1 405.5 |
| E43 | 12.6 | 608.0 | 7 311.0 | 603.3 | 6 161.0 | 792.8 | 3 030.7 | 648.1 | 1 482.9 |
| E53 | 13.0 | 641.1 | 9 092.0 | 569.5 | 8 813.4 | 774.6 | 3 451.6 | 687.9 | 1 823.0 |
| E71 | 13.1 | 597.8 | 7 425.5 | 562.6 | 6 829.1 | 755.8 | 3 005.5 | 645.1 | 1 524.0 |
| E93 | 14.4 | 639.2 | 8 688.9 | 614.3 | 7 836.4 | 830.9 | 3 410.5 | 709.4 | 1 700.1 |
| **Average** | **12.8** | **578.9** | **7 780.5** | **572.4** | **7 627.9** | **750.7** | **3 156.9** | **608.7** | **1 522.7** |

Table. IV Differences of weight, frequency and dynamic modulus in the wet-dry cycle

Initial results obtained during the last test before wetting should be obtained, and differences should have tended to 0, but the average difference obtained was 12% for frequencies and 30% for modulus. Because of these results and as the slope of variation was low, the process was accelerated by leaving the specimens in an oven at 105 ° for 24 hours.

### *1. Calculation of the evaporation coefficient*

To determine the equivalence of "drying" time, between that of a specimen stored in a temperate atmosphere and one stored in an oven, the extrapolation of results using trend curves of weight change (Fig. 10) over time can be used.

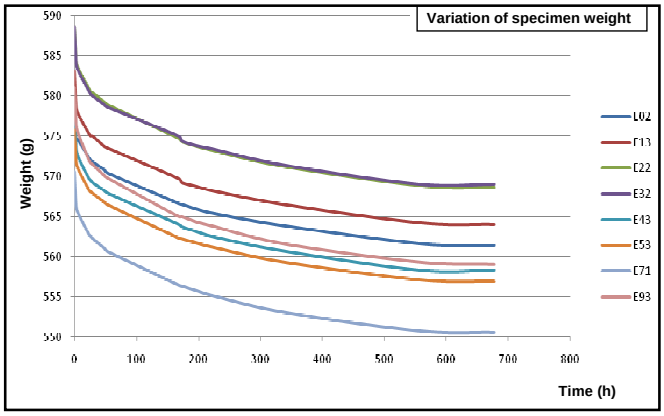


Fig. 10 Variation of specimen weight according to time

The evaporation coefficient, representing the wetting loss per hour (g / h), is calculated using the difference of time and weight between two consecutive tests. The graph below (Fig. 11) illustrates the curve of the evaporation coefficient for specimen E02 (the form and trend are the same for all other specimens).

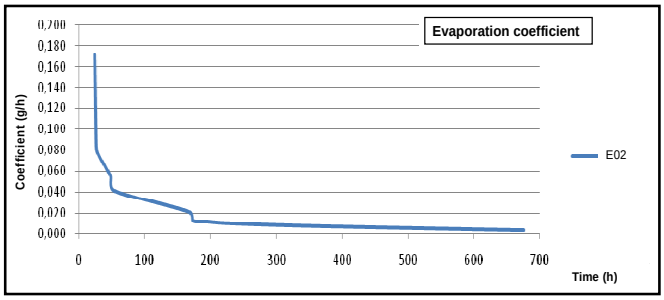


Fig. 11 Change in evaporation coefficient for specimen E02

The graph shows a sharp decrease in values until the 200$^{th}$ day; this because all the water molecules near the surface evaporates rapidly. Over time, they have to traverse a significant distance before reaching the surface in contact with air, resulting in a stabilization of the curve.

Once the coefficient is found, it is possible to deduce the number of equivalent hours (Table. V) using the weight loss of specimens before and after being put in the oven. The number of days may seem large, but the results seem consistent with the trend of the curves between the 600th and the 700th hour.

| Specimen | Coefficient | Equivalent hours | Equivalent days |
|---|---|---|---|
| E02 | 0.00819 | 2 320 | 97 |
| E13 | 0.00890 | 2 023 | 84 |
| E22 | 0.00943 | 1 993 | 83 |
| E32 | 0.00918 | 2 026 | 84 |
| E43 | 0.00915 | 1 858 | 77 |
| E53 | 0.00895 | 1 989 | 83 |
| E71 | 0.00939 | 1 895 | 79 |
| E93 | 0.01054 | 1 745 | 73 |

Table. V Equivalent hours and days corresponding to the evaporation coefficient

### *2. Dry-wet comparison*

The results from the dry and the wet phases are compared in order to determine the impact of intensive wetting of the specimens. For each series, the three criteria of weight, frequency and modulus are compared.

**Weight**

The following table (Table. VI) summarizes the comparison of weight before and after wetting.

The weight of the specimens increases by an average of 32 g - an average water absorption ratio of 0.12 g water / $cm^3$ mortar

| Specimen | Test | Weight (g) | | |
|---|---|---|---|---|
| | | | Difference (g) | Difference (%) |
| E02 | Before | 549.50 | 29.80 | 5.42 |
| | After | 579.30 | | |
| E13 | Before | 552.10 | 31.00 | 5.61 |
| | After | 583.10 | | |
| E22 | Before | 556.00 | 32.60 | 5.86 |
| | After | 588.60 | | |
| E32 | Before | 556.30 | 32.30 | 5.81 |
| | After | 588.60 | | |
| E43 | Before | 545.70 | 31.90 | 5.85 |
| | After | 577.60 | | |
| E53 | Before | 543.90 | 31.90 | 5.87 |
| | After | 575.80 | | |
| E71 | Before | 537.50 | 33.10 | 6.16 |
| | After | 570.60 | | |
| E93 | Before | 544.60 | 36.50 | 6.70 |
| | After | 581.10 | | |
| **Average** | | | **32.39** | **5.91** |
| **Standard deviation** | | | **1.95** | **0.38** |

Table. VI Comparison of weight before and after wetting

Except for specimens E32, E43 and E53, the weight gain (Fig. 12) is in constant increase and depends on the porosity.

The curves of variation in weight and of porosity accessible to water have the same appearance (increase, decrease, increase) except for the E3 series, which gives higher values than the E9 series.

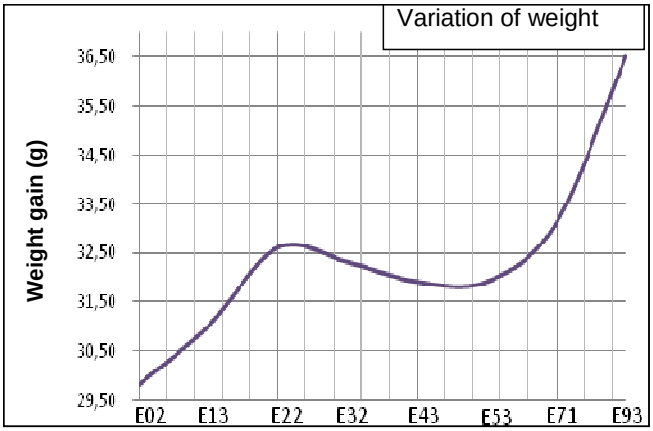


Fig. 12 Specimens' weight gain after 14 days

**Frequency and modulus**

The study of the influence of immersing the specimens for 14 days on frequency and modulus in four directions shows that the frequency increase is between 12 and 14% and for the modulus it is between 33 and 38%. This variation is very high for the longitudinal test.

Variations of modulus difference are similar in percentage (Fig. 13) for all tests (bending, torsion etc.)

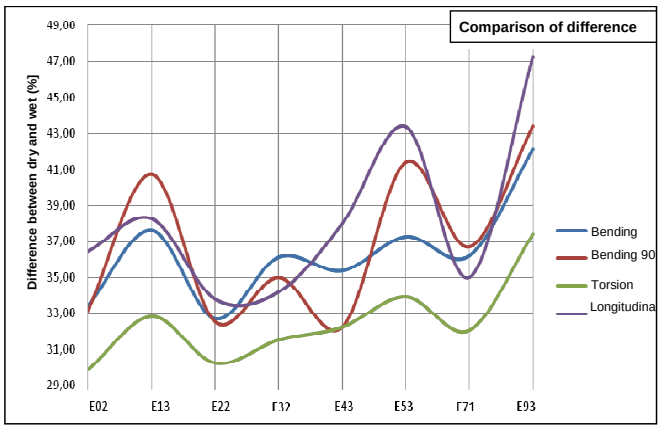


Fig. 13 Changes in the differences in modulus between the dry and wet phases

This comparison justifies the non-coherence of a test: for example, the results of bending 90 test on the specimen E43 does not give the same result as for the other three curves, where the tendency is either to increase or to stagnate; the dynamic modulus of specimen E43 loses more than 1 GPa: a sharp decrease.

From the above table (Tab 7) one can note that:

- Only 28 MPa separates the differences before and after wetting between specimen E43 and E02; this is low compared to the modulus obtained in 2 states (respectively 11.8 and 15.6 GPa).

- For the same specimens on the bending 90 test, the modulus differences between wet and dry are more than 1.300 MPa.

-The modulus difference between the reference specimen and any wet test will be negative or positive. More precisely, in half of the cases, it will be greater than that between the reference and the dry test.

The conclusion is that it is difficult (or impossible) to extend the numerical results identified on dried specimens to the same specimens when saturated with water.

### *3. Drying phase*

To study the behaviour of specimens in their drying phase, the results of each series of test are compared. As the tests were performed with one specimen for each series, the assumption is that the specimen is representative of the series.

From the graphs of the bending dynamic modulus (Fig. 14) and shear dynamic modulus (Fig. 15), we note:

- A reduction in the modulus of between 1.5 and 2 GPa in the first 24 hours, after which the slope of the curve decreases,

stabilizing at around the 700th hour.

- Except for specimen E43 which is similar to series 7 and 9, the three groups defined above (E0 & E2, E3 & E4 & E1 & E5, E7 & E9) reappear.

- The best linear results are those obtained in the torsion test; the least linear are those obtained in the longitudinal test.

- For all tests, a disparity of results appeared in hours 168 and 197. The variation in modulus (increase or decrease depending on the specimen) is difficult to explain. It may be due to the rapid decrease in the rate of evaporation of water present in the specimens (divided by 2 between hours 168 and 173), but it does not depend on the environmental conditions of storage, because the actual variation is also present in the dry-wet test while the specimens are immersed in water (H = 100%) between two measurements.

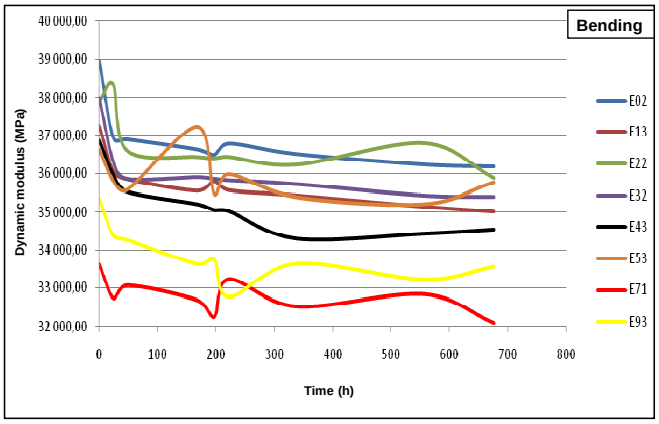


Fig. 14 Change in dynamic modulus in bending

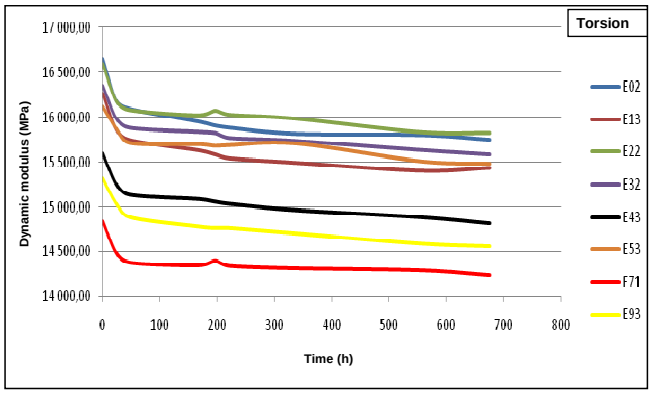


Fig. 15 Change in dynamic shear modulus

Changes in the weight and the dynamic shear modulus from the manufacture of the specimen until the end of the wet-dry test are represented respectively in Fig. 16 and Fig. 17.

In both cases the curves can be divided into three zones:

- The blue area represents the mortar with a more or less constant weight loss due to the evaporation of water which has not served to wet the cement. There is also an increase in shear modulus related to the hardening of mortar and the increase in its resistance. The two curves are almost symmetrical along the horizontal axis.

- The red zone represents the significant increase in weight and shear modulus when the specimen is immersed in water.

- The black area: during the drying of the specimens, the 2 curves are very similar. The slopes and shapes are identical and there is a decrease in weight and modulus over time based on the rate of water evaporation.

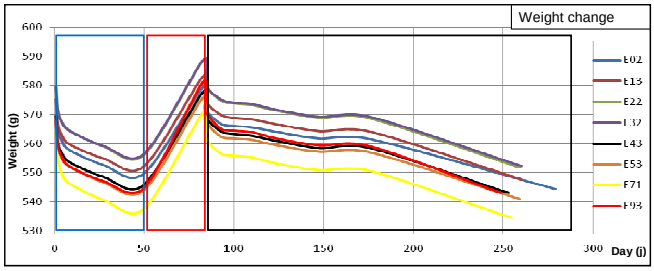


Fig. 16 Changes in dynamic bending modulus over a complete cycle

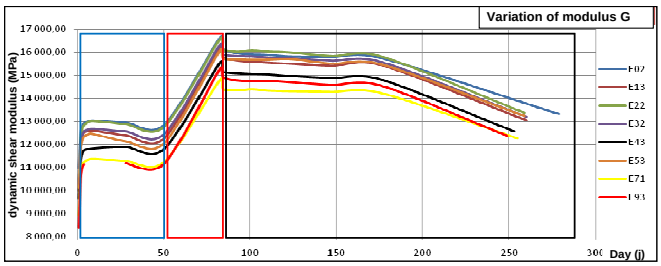


Fig. 17 Changes in dynamic shear modulus over a complete cycle

The results show that immersing a specimen in water for 14 days increases frequencies by about 13% and the modulus by about 35% for all tests (bending, torsion etc.). The dry-wet differences between the reference series and any other series are not quantitatively comparable, but it is possible to use the dry-wet comparison of the same series to check the validity of measures.

A sharp drop in dynamic modulus is observed for 24 hours after removal of the specimens from the water and then a lower and even more constant change of direction. Except for series E4, the groups of specimens defined above reappear in the wet-dry testing.

### *D. Dry-wet cycle*

To study a series of tests on a wet-dry cycle, the specimens were immersed in a tub filled with water and stored in a confined room with a constant temperature (≈20°C). To obtain uniform wetting on all surfaces, the specimens were placed on a metal grid in a water tank which was closed throughout the wetting cycle to prevent evaporation.

During the first three days after immersion, measurements were taken twice every 24 hours. It was possible to estimate the number of steps per day and per week (Fig. 18) to study the phenomenon. Changes in weight, frequency and modulus are greatest during the first days of wetting.

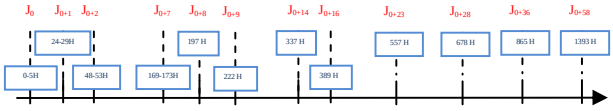

Fig. 18 Dates of measurements in the dry/wet cycle

Tests and measurements in the dry-wet cycle were performed on one specimen only of each series. With these measurements, it was possible to study the changes in specimen weight over time.

### *1. Changes in the weight of the specimens over the wetting period*

The following figure (Fig. 19) shows the variation of specimen weight over time

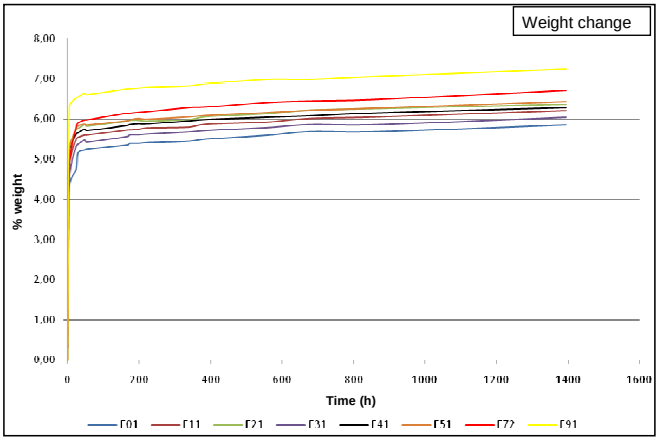


Fig. 19 Changes in specimen weight over the wetting period

It is seen that:
- There is a strong increase in weight during the first 24 hours of wetting. From the 48th hour, the increase in weight over time (slope of the curve) is lower and almost constant.
- There is a small disturbance in the curve between the 48th and the 53rd hour and also between the 169th and the 173rd hour of immersion.
- The weight increase is not proportional to the increase of porosity in the specimens: weight gain of specimen E31 is lower than that of specimen E11 and E21 which have, respectively, weight gains similar to E41 and E51 (Table. VII). This can be explained by the more or less closed porosity of each specimen.

| Specimen | Weight gain | |
|---|---|---|
| | (g) | (%) |
| E01 | 32 | 5.84 |
| E11 | 34.6 | 6.22 |
| E21 | 35.1 | 6.37 |
| E31 | 33.5 | 6.04 |
| E41 | 34.4 | 6.28 |
| E51 | 35.2 | 6.43 |
| E72 | 35.8 | 6.70 |
| E91 | 39.8 | 7.24 |

Table. VII Weight gain in specimens

According to the curve of percentage change in total weight (Fig. 20), for a gradual increase in weight compared to an increase in the porosity of the specimens (best curve fitting), the measurements made on specimen E11, E21 and E31 or a measure of total porosity should be reassessed.

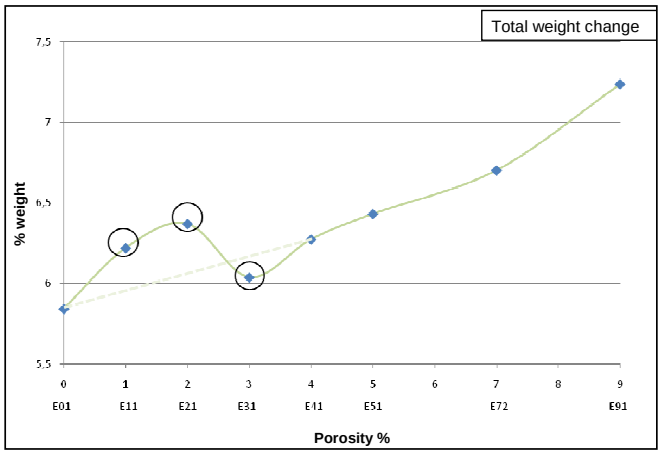


Fig. 20 Percentage change in total weight

### *2. Change in specimens' dynamic modulus over the wetting period*

Figures 21 and 22 represent the dynamic modulus curves for bending and torsion; they are used to analyze the previous results.
There is a correlation between the immersion of specimens in water and the increasing dynamic modulus: the shape of the "dynamic modulus / time" curve is similar to the shape of the curve "percentage weight / time".
The main increase in dynamic modulus occurs during the first two days (until the 53rd hour); then, between the 53rd and 169th hour of immersion, there is a transition period where the slope of the curve starts to stabilize, and finally the increase of dynamic modulus over time (slope of the curve) is almost constant from the 169th hour.

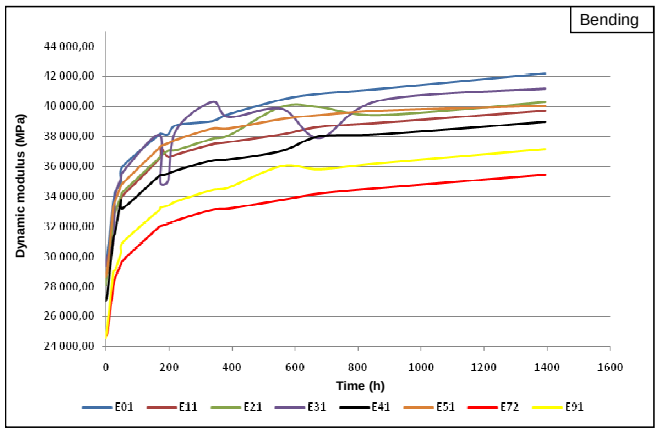


Fig. 21 Dynamic modulus in bending

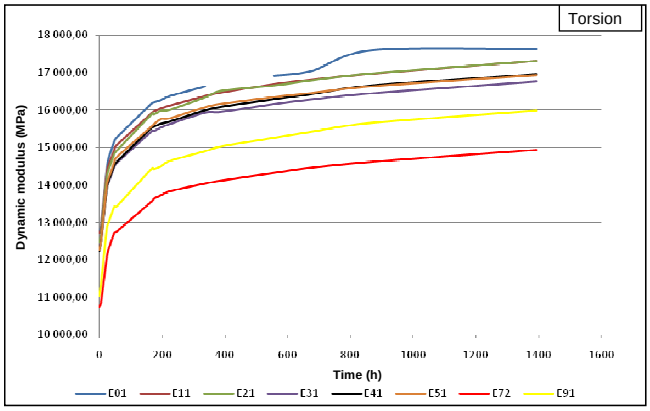

Fig. 22 Dynamic modulus in torsion

Despite the similarity of the "dynamic modulus / time" and "percentage weight / time" curves, there is a lag between the time taken for the slopes of the curves to stabilize; the slope of the "percentage weight / time" curve starts to stabilize from the 48th hour while that of "dynamic modulus / time" starts to stabilize from the 169th hour.

There is no correspondence between the values of dynamic modulus and the porosity of the specimens, for example specimen E72.

There are many disturbances in all specimens between the 48th and the 53rd hour and also between the 169th and the 173rd hour of immersion. During these periods, there are disturbances in the increase in weight of specimens, more visible on the unstable specimens E21 and E31.

To deepen the analysis, the total change (between day 0 / hour 0 and day 58 / hour 1393) in dynamic modulus for the cycle of wetting for each test specimen was treated for resonance modes in bending and torsion (Fig. 23).

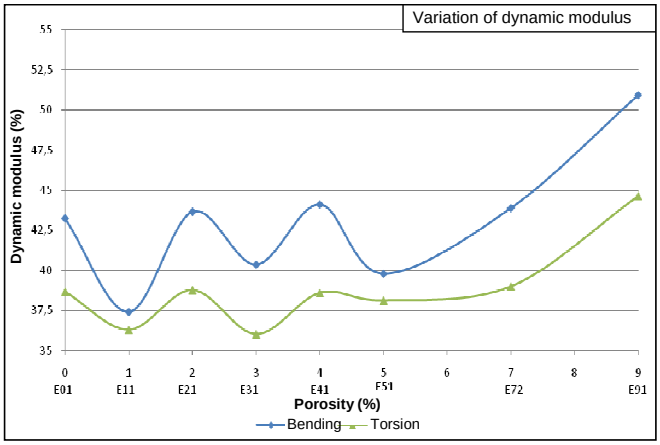

Fig. 23 Percentage variation of dynamic modulus

According to the results, there is a rather irregular increase in modulus between specimens. It is neither constant nor proportional to the increase in weight of specimens. There are specimens with a low degree of porosity but with a greater variation of dynamic modulus than that of another series with a higher level of porosity. These disparities of dynamic modulus between specimen shows that the wetting cycle disrupts the consolidation of the specimens. Qualitatively, the two curves follow the same path.

### *3. Dynamic modulus average between specimens*

To analyze the modulus average over a complete cycle from manufacture until the end of wetting cycle, curves are plotted and the values of the average deviations are compared in order to decide on / determine the influence that the cycle of wetting may have on the analysis of structural damage.

For the bending test (Fig. 24), two zones can be differentiated: the first corresponds to the phase before wetting, with a sharp rise in dynamic modulus due to the inclusion of mortar; after this sharp rise, the dynamic modulus remains constant in most specimens. The second zone is the dry–wet cycle, in which the curves fail to reach a threshold value and they continue to rise over time. For both zones, there is a sharp rise in dynamic modulus corresponding, respectively, to the mortar and the first days of wetting.

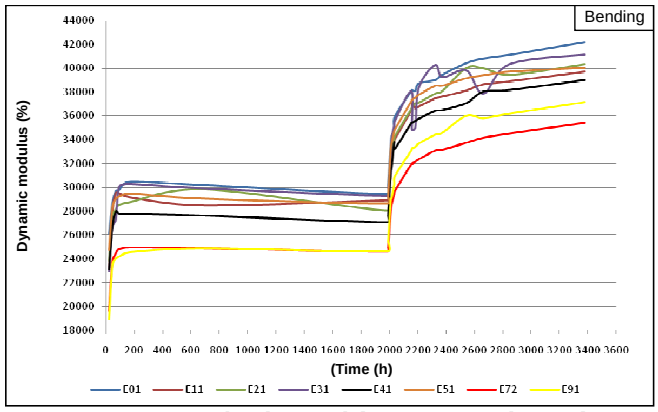

Fig. 24 Dynamic bending modulus over a complete cycle

The curves of specimens E21 and E31 are the most incoherent. In the first phase, E21 already had unstable behaviour that intensified during the wetting cycle, unlike specimen E31, where instability is delayed beyond the beginning of the wetting cycle. It was noted that E31 also had unstable behaviour in two other directions of vibration: bending 90 and longitudinal.

The wetting cycle tends to accentuate and intensify unstable behaviour of specimens. This may be due to the interaction of water in a non-homogeneous structure (solid mixture and vacuum) inside the mortar.

In torsion there are also two zones in the "dynamic modulus / time" curve (Fig. 25). The behaviour of the specimens is very stable before and after humidification. This curve shows that there is an increasing gap between specimens. It was possible to group (before the wetting cycle) different specimens according to their thresholds of "dynamic modulus / porosity". This grouping was used to validate the interest of the diffuse damage analysis using the vibration signature. The wetting cycle and has an interest that the identification of diffuse damage in the structure through the frequencies become easy. When the differences are larger, the identification of a diffuse damage due to dynamic modules does not require grouping of specimens based on thresholds of porosity. For example, in a

cycle of wetting, it is more accurate to identify the diffuse damage (percentage porosity) between specimens E72 and E91 through their dynamic modulus.

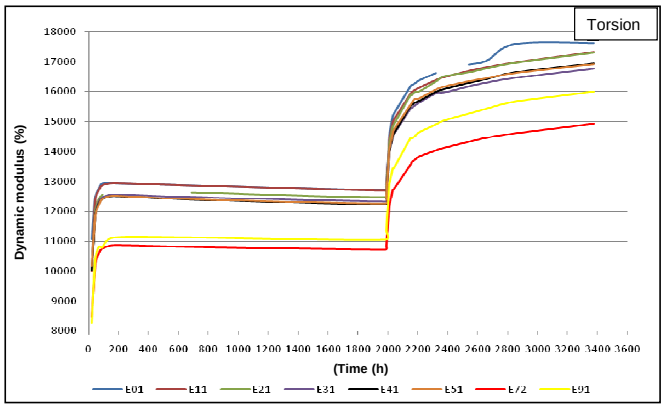


Fig. 25 Dynamic shear modulus over a complete cycle

From the obtained results, wetting specimens produced a large increase in weight during the first 24 hours (from the 48th hour the weight gain becomes smaller and more constant). It generates a large increase in dynamic modulus during the first 48 hours and a steady increase from the 169th hour. It is possible to correlate the hypothesis that the increased weight due to specimen wetting (presence of water in pores) causes an increase in dynamic modulus. For specimens E11, E21 and E31, the increase in weight and dynamic modulus are not proportional to the rate of porosity.

The dry-wet cycle increases or causes instability in the vibration modes of some specimens. This destabilization disrupts the use of vibration signature analysis for diffuse damage.

Despite this instability, the cycle of wetting has an advantage in the analysis of diffuse damage. It increases the gap between the modulus of the different specimens (different levels of mortar porosity). This feature can help better identify diffuse damage using the vibration signature.

## V. Conclusion

This study has shown that cycles of wetting and drying disrupt the stability of the measurements made with GrindoSonic. The cycle of wetting and drying allows better analysis and validation of the results found for diffuse damage and it greatly increases the dynamic modulus of specimens during the first 48 hours. The drying cycle does not change the results of the diffuse damage to the specimens. The amount of water present in specimens modifies their behavior during a dynamic impact.

The vibration signature permits the quantification of diffuse damage on specimens using a threshold of porosity, and to qualify located damage.

The instability of some series of measurements is evidence (although they have yet to be demonstrated on other equivalent specimens) of the limits of GrindoSonic.

The increase in specimens' weight (presence of additional water) during the wetting tests amplified increased the dynamic modulus, although no direct relationship was found. The rise in / increase in of the modulus is not proportional to weight gain.

The dynamic modulus is significantly influenced by the crack characteristics, and this influence varies according to the test.

It is important to perform all the tests - bending, bending 90, longitudinal and torsion - because even if they are not well-suited to a particular type of defect, they can still be used to check the consistency of other results.

It is hoped that the present study will validate this approach through the establishment of a numerical model of the specimens designed to find the frequencies and dynamic modulus defined using GrindoSonic. The approach will then be applied to a reinforced concrete structure such as a beam or plate.

## References

[1] *BSyISO 15686 Buildings and Constructed Assets – Service Life Planning–Part 1: General Principle*, British Standards Institution, London, 2000.

[2] D. Doran, "New standard for service-life planning". *Struct Eng*, vol. 19, no. 78. pp. 8, 2000

[3] L.U. Litzner, "Eurocode 2-Innovations in design and construction of concrete structures", *In: R.K. Dhir. M.R. Jones (eds.), Proceedings Creating with Concrete Conference*, London: Thomas Telford Ltd, 2000, pp. 193–209

[4] X. Tao, D.V. Phillips, "A simplified isotropic damage model for concrete under bi-axial stress states", *Cement and Concrete Composites*, vol. 27, no. 6, pp. 716-726, 2005.

[5] A. Cimetière, D. Halm, E. Molines, "A damage model for concrete beams in compression", *Mechanics Research Communications*, vol. 34, no. 2, pp. 91-96, 2007.

[6] A. Alliche, "Damage model for fatigue loading of concrete", *International Journal of Fatigue*, vol. 26, no. 9, pp. 915-921, 2004

[7] J. Mazars, " Application de la mécanique de l'endommagement au comportement non linéaire et à a rupture du béton de structure", Thesis report, Paris 6, 1984.

[8] L.M. Kachanov, "Time of the rupture process under creep conditions", *Izv. Akad. Nauk. S.S.R Otd Tekh Naut*, no. 8, pp. 26-31, 1958.

[9] N. Baghiee, M. R. Esfahani, K. Moslem, "Studies on damage and FRP strengthening of reinforced concrete beams by vibration monitoring", *Engineering Structures*, vol. 31, no. 4, pp. 875-893, 2009.

[10] Z. Zembaty, M. Kowalski, S. Pospisil, "Dynamic identification of a reinforced concrete frame in progressive states of damage", *Engineering Structures*, vol. 28, no. 5, pp. 668-681, 2006.

[11] J. M. Ndambi, J. Vantomme, K. Harri, "Damage assessment in reinforced concrete beams using eigenfrequencies and mode shape derivatives", *Engineering Structures*, vol. 24, no. 4, pp. 501-515, 2002

[12] L. Zheng, X. Sharon Huo, Y. Yuan, "Experimental investigation on dynamic properties of rubberized concrete", *Construction and Building Materials*, vol. 22, no. 5, pp. 939-947, 2008.

[13] J. Maeck et al, "Damage identification in reinforced concrete structures by dynamic stiffness determination", *Engineering Structures*, vol. 22, no. 10, pp. 1339-1349, 2000.

[14] P. Antonaci et al, "Monitoring evolution of compressive damage in concrete with linear and nonlinear ultrasonic methods", *Cement and Concrete Research*, vol. 40, no. 7, pp. 1106-1113, 2010.

[15] J.F. Chaix, V. Garnier, G. Corneloup, "Concrete damage evolution analysis by backscattered ultrasonic waves", *NDT & E International*, vol. 36, no. 7, pp. 461-469, 2003.

[16] D. Breysse et al, "How to combine several non-destructive techniques for a better assessment of concrete structures", *Cement and Concrete Research*, vol. 38, no. 6, pp. 783-793, 2008.

[17] A.M. Neville, *Properties of Concrete (Fourth and Final ed.)*, John Wiley & Sons, New York, 1996.

[18] J. M. Reynouard, G.P. Cabot, *Comportement mécanique du béton*, Editions Lavoisier, Paris, 2005.
[19] B. Zhang, "Relationship between pore structure and mechanical properties of ordinary concrete under bending fatigue", *Cement and Concrete Research*, vol. 28, no. 5, pp. 699–711, 1998.
[20] C. Payan, V. Garnier, J. Moysan, "Effect of water saturation and porosity on the nonlinear elastic response of concrete", *Cement and Concrete Research*, vol. 40, no. 3, pp. 473-47, 2010.
[21] R. Schmidt, V. Wicher, R. Tilgner, "Young's modulus of moulding compounds measured with a resonance method", *Polymer Testing*, 2, vol. 24, no. 2, pp. 197-203, 2005.
[22] H. Wang, Q. Li, "Prediction of elastic modulus and Poisson's ratio for unsaturated concrete", *International Journal of Solids and Structures*, vol.44, no.5, pp. 1370-1379, 2007.
[23] *GrindoSonic instrument*, available from Lemmens-Electronika, N.V. Leuven, Belgium.
[24] *C1259-01: Standard test method for dynamic young's modulus, Shear modulus and Poisson's ratio for advanced ceramics by impulse excitation of vibration*, ASTM, 2001.
[25] *NF EN 196-1. 1995 NF EN 196-1, Méthode d'essais des ciments, Partie 1: Détermination des résistances mécaniques*, 1995
[26] *NBN-B 15-230 : Essais non destructifs - Mesure de la fréquence de résonnance*, Institut Belge de normalisation, 1976.